

# From Non-interacting to Interacting Picture of Thermodynamics and Transport Coefficients for Quark Gluon Plasma

Sarthak Satapathy<sup>\*</sup>, Souvik Paul<sup>†, \*</sup>, Ankit Anand<sup>†, \*</sup>, Ranjesh Kumar<sup>†, \*</sup>,  
Sabyasachi Ghosh<sup>\*</sup>

<sup>\*</sup>Indian Institute of Technology Bhilai, GEC Campus, Sejabhar, Raipur 492015,  
Chhattisgarh, India

<sup>†</sup> Department of Physical Sciences, Indian Institute of Science Education and Research  
Kolkata, Mohanpur, West Bengal 741246, India

## Abstract

We have attempted to build first some simplified model to map the interaction of quarks and gluons, which can be contained by their thermodynamical quantity like entropy density, obtained from calculation of lattice quantum chromo dynamics (LQCD). With respect to entropy density of the standard non-interacting massless quark gluon plasma (QGP), its interacting values from LQCD simulation are reduced as we go from higher to lower temperature through the cross-over of quark-hadron phase transition. By parameterizing increasing degeneracy factor or increasing interaction-fugacity or decreasing thermal width of quarks and gluons with temperature, we have matched LQCD data. Using that interaction picture, shear viscosity and electrical conductivity are calculated. For getting nearly perfect fluid nature of QGP, interaction might have some role when we consider temperature dependent thermal width.

## 1 Introduction

Thermodynamics of quark gluon plasma (QGP) can be well described by lattice quantum chromodynamics (LQCD) calculation, which predicted a quark-hadron phase transition since a long time [1] and its numerical estimations have gone through several upgradation [2]. From the direction of perturbative quantum chromodynamics (QCD) theory, a re-summation method, known as hard thermal loop (HTL) approach, is well studied historically, whose latest status can be found in Ref. [3]. In this direction it is found that three loop order calculations of HTL perturbation theory [4, 5] can well describe the LQCD results of thermodynamics beyond the transition temperature. The finite density extension of this three loop calculations has been studied in Ref. [6, 7]. Similar to quark temperature domain, LQCD thermodynamics of hadronic temperature domain can be well described by simple ideal hadron resonance gas (HRG) model [8]. To describe the LQCD thermodynamics of both quark and hadronic temperature domain, there are very successful effective QCD models [9, 10, 11], which can explain the smooth cross-over results of quark-hadron transition. In this context, Quasi particle model (QPM) is a widely used framework [12, 13, 14, 15, 16, 17, 18, 19, 20, 21, 22] to describe the thermodynamics of

QGP through entire temperature zone. Some attempts [12, 13, 14, 15] made by incorporating temperature dependent masses of medium constituents, which become quite popular and standard. Ref. [16] has built a self-consistent equation, where gluon mass is considered as plasma frequency, depending upon density of the system. Refs. [20, 21, 22] have built interestingly a quasi-particle model by introducing effective fugacity parameter in thermal distribution functions of quarks and gluons. In present work, we have first followed the effective fugacity methodology, adopted by Refs. [20, 21, 22], and attempted to reproduce qualitatively an existing quasi-particle model. Then we have tried to find more alternative methodologies, which can match same LQCD thermodynamics. By comparing them, we have tried to extract some common qualitative message.

After building the different quasi-particle models to map the QCD interaction, provided by LQCD data, our next aim become to tune our models with experimental properties of QGP. The experimental data [23, 24] from heavy ion collision experiments like RHIC [23] at BNL, USA and LHC [24] at CERN, Switzerland indicate that QGP is a nearly perfect fluid system, which can be quantified by a very small values of shear viscosity to entropy density ratio  $\eta/s$ . The entropy density  $s$  of interacting QGP can already be known from LQCD direction, from where the strength of thermodynamical phase-space part of shear viscosity  $\eta$  can be fixed but it is relaxation time, which maps the collective dissipative properties of QGP. We have explored this fact in present article. Mapping the interacting QCD picture through different effective QCD models, Refs [25, 26, 27, 28, 29, 30, 31, 32, 35, 34, 33, 36, 37, 38] have addressed about the estimation of shear viscosity for quark matter. Whereas, different quasi-particle models [38, 39, 40, 41, 42, 43] provide the similar directional estimations. All those investigations have a common/main interest on searching some sources, for which QGP shows low viscous behavior. Here we have particularly focus on the role of interaction for reduction of viscosity and fluidity of the medium, where interaction picture have been built via three different simplified methodologies. We have also studied other transport coefficients like electrical conductivity of QGP.

The article is organized as follows. We have addressed the detail methodologies for building the quasi particle models in next Sec. (2), which are classified into three subsections - (2.1), (2.2) and (2.3) to describe three different alternative ways to map interaction picture. After mapping the interaction in the models, we have applied to estimate transport coefficients of QGP, which are discussed in Sec. (3) and at the end, we have summarized our investigation.

## 2 Thermodynamic models by parameterizing LQCD data

### 2.1 Temperature dependent degeneracy factor

Let us start with a non-interacting description of quark gluon plasma, where u, d, s quarks, their anti-quarks and 8 different gluons are in thermal equilibrium. So quarks and anti-quarks will follow Fermi-Dirac (FD) distribution and gluons obey Bose-Einstein (BE) distribution. Following standard framework of statistical mechanics, one can calculate energy density and pressure of QGP system as

$$\epsilon = g_g \int_0^\infty \frac{d^3 p}{(2\pi)^3} \frac{p}{e^{\beta p} - 1} + g_u \int_0^\infty \frac{d^3 p}{(2\pi)^3} \frac{\omega_u}{e^{\beta \omega_u} + 1} + g_s \int_0^\infty \frac{d^3 p}{(2\pi)^3} \frac{\omega_s}{e^{\beta \omega_s} + 1} \quad (1)$$

and

$$\begin{aligned} P &= g_g \int_0^\infty \frac{d^3 p}{(2\pi)^3} \left( \frac{p}{3} \right) \frac{1}{e^{\beta p} - 1} + g_u \int_0^\infty \frac{d^3 p}{(2\pi)^3} \left( \frac{p^2}{3\omega_u} \right) \frac{1}{e^{\beta \omega_u} + 1} \\ &+ g_s \int_0^\infty \frac{d^3 p}{(2\pi)^3} \left( \frac{p^2}{3\omega_s} \right) \frac{1}{e^{\beta \omega_s} + 1}, \end{aligned} \quad (2)$$

where  $\omega_u = \{p^2 + m_u^2\}^{1/2}$ ,  $\omega_s = \{p^2 + m_s^2\}^{1/2}$ , with  $m_u = 0.005$  GeV,  $m_s = 0.100$  GeV. The  $g_u$ ,  $g_s$  and  $g_g$  are degeneracy factor u, d quarks, s quark and gluon respectively. Their values are given below

$$\begin{aligned} g_u &= (\text{spin}) \times (\text{particle/anti particle}) \times (\text{color}) \times (\text{flavor}) = 2 \times 2 \times 3 \times 2 = 24, \\ g_s &= (\text{spin}) \times (\text{particle/anti particle}) \times (\text{color}) \times (\text{flavor}) = 2 \times 2 \times 3 \times 1 = 12, \\ g_g &= (\text{spin}) \times (\text{flavor}) = 2 \times 8 = 16. \end{aligned} \quad (3)$$

Using thermodynamical relation with zero quark (and obviously gluon) chemical potential of QGP system, we can obtain entropy density

$$s = \frac{P + \epsilon}{T}. \quad (4)$$

Using Eqs.(1), (2),  $s$  can be calculated and it will be very close to the analytic expression of Stephan-Boltzmann (SB) limit ( $m_{u,s} \approx 0$ ):

$$s = \left[ g_g + (g_u + g_s) \left( \frac{7}{8} \right) \right] \frac{4\pi^2}{90} T^3 \approx 20.8 T^3. \quad (5)$$

According to lattice Quantum Chromo Dynamics (LQCD) calculation [44, 45], the numerical values of  $s$  for QGP remain always lower than its SB limits, which indicates about interaction picture of the system. For visualization, see Fig. 1(b), which will elaborately discussed latter. Though LQCD is best tool to map the interaction of QGP system, based on the theory of quantum chromo dynamics (QCD) but one can map this interaction via simple quasi-particle model description. So, idea is to use simple and standard non-interacting thermodynamical relations, given in Eqs. (1), (2) and (4), where a temperature dependent interacting information will carry by some quantity of quarks and gluons. One can get a huge number of references [9, 10, 11, 12, 13, 14, 15], where interaction information is mainly captured by temperature dependent of masses of quarks and gluons. Here, we have caught the quantity degeneracy factors, whose temperature dependence can map the QCD interaction as an alternative and simplified way. From LQCD data [44, 45], we find that  $s$  decreases if we decrease the temperature ( $T$ ) and near the quark-hadron phase transition temperature ( $T_c$ ), its rate of decrement along -ve  $T$ -axis become maximum and at last in low temperature range, where QGP appears as hadronic degrees of freedom, the values of  $s$  becomes quite small. Now if one concentrate on hadronic temperature range ( $T < T_c$ ), and try to get LQCD values of  $s(T < T_c)$ , one of the immediate attempt comes through non-interacting hadronic matter (HM) calculation. Considering pion and Kaon as most abundant mesons with u, d and s quarks, one can estimate  $s(T < T_c)$  from the corresponding thermodynamical relations

$$\begin{aligned} s(T < T_c) &= g_\pi \int_0^\infty \frac{d^3 p}{(2\pi)^3} \left[ \omega_\pi + \frac{\vec{p}^2}{3\omega_\pi} \right] \frac{1}{e^{\beta \omega_\pi} + 1} \\ &+ g_K \int_0^\infty \frac{d^3 p}{(2\pi)^3} \left[ \omega_K + \frac{\vec{p}^2}{3\omega_K} \right] \frac{1}{e^{\beta \omega_K} + 1}, \end{aligned} \quad (6)$$

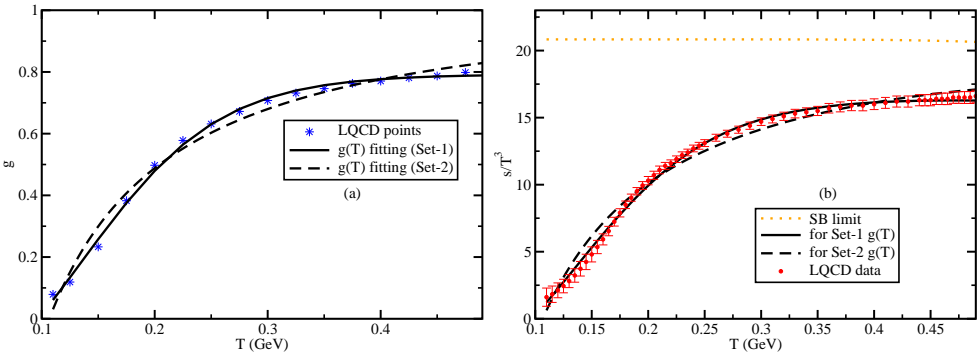


Figure 1: (a) Temperature dependence degeneracy factors  $g(T)$  parametrization curves - Set-1 (solid line), Set-2 (dash line) and LQCD extracted points (stars). (b) Their corresponding  $s/T^3$  plots, where straight horizontal dotted line indicates SB limits of  $s/T^3$ .

where  $\omega_\pi = \{\vec{p}^2 + m_\pi^2\}^{1/2}$ ,  $\omega_K = \{\vec{p}^2 + m_K^2\}^{1/2}$  with  $m_\pi \approx 0.140$  GeV and  $m_K = 0.500$  GeV and degeneracy factors of pion and kaon are  $g_\pi = 3$  and  $g_K = 4$ . The numerical values of Eq. (6) will be little below than its SB limits

$$s(T < T_c) = (g_\pi + g_K) \frac{4\pi^2}{90} T^3 \approx 3 T^3. \quad (7)$$

The numbers of  $s(T < T_c)$  in this simple non-interacting picture of HM system is quite close to LQCD data around low temperature range of hadronic phase. So non-interacting QGP and HM system provide us upper and lower estimations of  $s$ , within which LQCD data points [44, 45] are located, where major changes in values of  $s$  (or any other thermodynamical quantities) are occurred near  $T_c$ . There are famous hadron reason gas (HRG) model [8], which can match LQCD data exactly for  $T \leq T_c$  range. Some Refs. [4, 5, 16] can cover the  $T \geq T_c$  range. While quasi-particle based Refs. [9, 10, 11, 20, 21, 22] attempted to span both temperature range  $T \leq T_c$  and  $T \geq T_c$  with QGP system, where  $T \leq T_c$  zone basically tell about quasi particle nature of quarks and gluons inside hadrons. Here we also try to build that kind of quasi-particle identities of quarks and gluons through entire temperature range. From simplified non-interacting picture, we get a guidance that during the transition from quark to hadronic matter the degeneracy factors has abruptly reduced from  $(g_u, g_s, g_g)$  set to  $(g_\pi, g_K)$  set, for which  $s/T^3$  is reduced from 20.8 to 3. Now LQCD data is saying that this reduction is not abruptly like first order phase transition rather smoothly like a cross-over transition. By assuming appropriate temperature dependent degeneracy factors of quarks and gluons, one can construct LQCD data points for  $s(T)$ . For this purpose, we have considered a temperature dependent factor  $g(T)$ , attached with  $g_{q,s,g}$  and then match the LQCD data of  $s(T)$  [44, 45]. We get a parametrized expression:

$$g(T) = a_0 - \frac{a_1}{e^{a_2(T-a_3)} + a_4}, \quad (8)$$

where  $a_0 = 0.793$ ,  $a_1 = 0.687$ ,  $a_2 = 16.284$ ,  $a_3 = 0.170$ ,  $a_4 = 0.560$ . The above set of parameters (say set-1) provide better matching to LQCD data but it is not satisfying the expectation of reaching SB limit of  $s$  at  $T \rightarrow \infty$ . To fulfill the condition, we have restricted

$a_0 = 1$ , and get the another parametrized function:

$$g(T) = 1 - \frac{b_0}{e^{b_1(T-b_2)} + b_3} , \quad (9)$$

where  $b_0 = 0.793$ ,  $b_1 = 0.687$ ,  $b_2 = 0.170$ ,  $b_3 = 16.284$ , which can be called set-2.

Fig. 1(a) shows two set of  $g(T)$  (dash and solid lines) and LQCD data points (stars) [44, 45]. Their corresponding values of  $s/T^3$  is plotted in Fig. 1(b), where SB limit denoted by straight horizontal dotted line. So effectively total degeneracy factor of QGP  $g_u + g_s + g_g = 52$  will be suppressed for considering  $g(T) * g_{u,s,g}$ , and around  $T = 0.200$  GeV,  $g(T) \approx 0.5$ , which means effective degeneracy factor become  $0.5 \times 52 = 26$ . In hadronic temperature range, around  $T \approx 0.120$  GeV,  $g(T) \approx 0.13$  will provide effective degeneracy factor  $0.13 \times 52 = 7$ , which is exactly hadronic degeneracy factor  $g_\pi + g_K = 7$ . So in this way, we might roughly map QCD interaction picture via shrinking of degeneracy factor of quarks and gluons with lowering the temperature. This fact can be compared with the fact of temperature dependent degree of freedom for di-atomic or n-atomic molecule. At low temperature degrees of freedoms of di-atomic or n-atomic molecules is  $3 \times 2 - 1$  or  $3 \times n - k$  because of its 1 or  $k$  number of atomic bondings, which can be broken at high temperature and degrees of freedom enhanced as

$$\begin{aligned} 3 \times 2 - 1 &= 5 \rightarrow 3 \times 2 = 6 \\ \text{or,} \\ 3 \times n - k &\rightarrow 3 \times n . \end{aligned} \quad (10)$$

According to equipartition theorem of thermodynamics, internal energy of di-atomic or n-atomic molecular system will be proportional to its degrees of freedom, hence internal energy (other thermodynamical quantities) will also be increased with increasing temperature.

## 2.2 Temperature dependent Fugacity

As an alternative method, instead of temperature dependent degeneracy factors of quarks and gluons, one can mimic QCD interaction via temperature dependent fugacity  $Z(T)$ , as addressed in quasi-particle model of Chandra-Ravisankar [20, 21, 22]. This fugacity quantity is just for mimicking the QCD interaction but should not be confused with fugacity  $Z_{q,g} = \exp(\mu_{q,g}/T)$  due to quark/gluon chemical potential, which are considered as zero for present system. Hence, to get interacting values of  $\epsilon$  and  $P$ , we have to replace  $e^{\beta p}$ ,  $e^{\beta \omega_u}$  and  $e^{\beta \omega_s}$  in Eqs. (1), (2) by  $Z^{-1}e^{\beta p}$ ,  $Z^{-1}e^{\beta \omega_u}$  and  $Z^{-1}e^{\beta \omega_s}$ , as we are considering modified thermal distribution functions of u/d quark, s quark and gluon as

$$\begin{aligned} f_u &= \frac{1}{Z^{-1}\exp(\beta\sqrt{p^2 + m_u^2}) + 1} \\ f_s &= \frac{1}{Z^{-1}\exp(\beta\sqrt{p^2 + m_s^2}) + 1} \\ f_g &= \frac{1}{Z^{-1}\exp(\beta p) - 1} . \end{aligned} \quad (11)$$

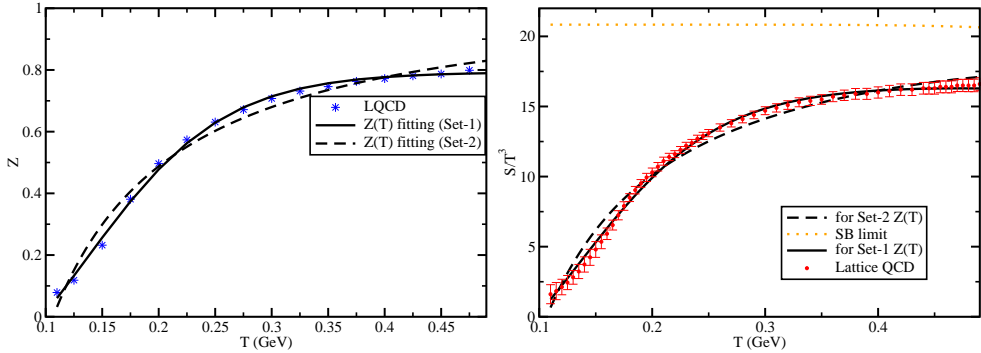


Figure 2: (a) Temperature dependence fugacity  $Z(T)$  parametrization curves - Set-1 (solid line), Set-2 (dash line) and LQCD extracted points (stars). (b) Their corresponding  $s/T^3$  plots, where straight horizontal dotted line indicates SB limits of  $s/T^3$ .

After knowing  $\epsilon$ ,  $P$ ,  $s$  can be obtained from Eq. (4). Keeping  $Z$  as tuning parameter, we have matched the LQCD data [44, 45] of  $s$  and we get a parametrized form

$$Z(T) = a_0 - \frac{a_1}{e^{a_2(T-a_3)} + a_4}, \quad (12)$$

Where  $a_0 = 0.792535$ ,  $a_1 = 0.686132$ ,  $a_2 = 16.2834$ ,  $a_3 = 0.170$   $a_4 = 0.56037$  At  $T \rightarrow \infty$ ,  $Z \rightarrow a_0$ , which is 0.792535 but not 1. It means that this set (say set-1) is not fulfilling the expectation of getting non-interacting picture at high temperature limit. Therefore, restricting  $a_0 = 1$ , we find another parametrized form

$$Z = 1 - \frac{b_0}{e^{b_1(T-b_2)} + b_3} \quad (13)$$

Where  $b_0 = 0.138935$ ,  $b_1 = 1.445$ ,  $b_2 = 0.170$   $b_3 = -0.77362$  (say set-2) and the expectation  $Z(T \rightarrow \infty) \rightarrow 1$  is well satisfied. These two sets of  $Z(T)$  are shown by dash and solid curves in Fig. 2(a), where stars are LQCD data extracted points of  $Z$ . Their corresponding values of  $s/T^3$  is plotted in Fig. 2(b), where SB limit denoted by straight horizontal dotted line.

### 2.3 Temperature dependent Thermal width

Here, we will explore another alternative possibility to building a quasi-particle model via temperature dependent thermal width of quarks and gluons. For this purpose, let us revisit Eq. (1) and re-write in other way:

$$\begin{aligned} \epsilon &= g_g \int_0^\infty dM \delta(M) \int_0^\infty \frac{d^3p}{(2\pi)^3} \frac{\sqrt{p^2 + M^2}}{\exp(\beta\sqrt{p^2 + M^2}) - 1} \\ &+ g_u \int_0^\infty dM \delta(M - m_u) \int_0^\infty \frac{d^3p}{(2\pi)^3} \frac{\sqrt{p^2 + M^2}}{\exp(\beta\sqrt{p^2 + M^2}) + 1} \\ &+ g_s \int_0^\infty dM \delta(M - m_s) \int_0^\infty \frac{d^3p}{(2\pi)^3} \frac{\sqrt{p^2 + M^2}}{\exp(\beta\sqrt{p^2 + M^2}) + 1}, \end{aligned} \quad (14)$$

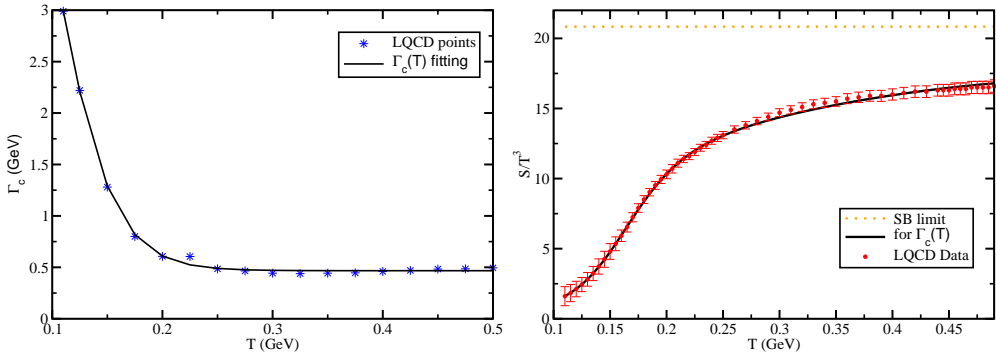


Figure 3: (a) Temperature dependence thermal width  $\Gamma_c(T)$  parametrization curve (solid line) and LQCD extracted points (stars). (b) Their corresponding  $s/T^3$  plots, where straight horizontal dotted line indicates SB limits of  $s/T^3$ .

which is exactly same as Eq. (1), after using the identity  $\int \delta(x - x_0) f(x) dx = f(x_0)$ . In non-interacting picture, quarks and gluons are stable and having delta function profile in mass space, but for interacting case, delta function can be converted to Breit Weigner function

$$\rho(M) = \frac{1}{\pi} \left( \frac{\Gamma_c}{\Gamma_c^2 + (M - M_0)^2} \right), \quad (15)$$

where  $M, M_0$  is off-shell, on-shell mass of particle and  $\Gamma_c$  is thermal width of the particle, which basically maps the collision picture. One can get back delta distribution for vanishing thermal width because of relation

$$\delta(M - M_0) = \lim_{\Gamma_c \rightarrow 0} \rho(M). \quad (16)$$

The transition from non-interacting to interacting picture via  $\delta(M - M_0) \rightarrow \rho(M)$  in energy/momentum space will be more clear through the transition  $1 \rightarrow e^{-t/\tau_c}$  or  $1 \rightarrow e^{-x/\lambda_c}$  in time/position space, where  $\tau_c = 1/\Gamma_c$  or  $\lambda_c \propto 1/\Gamma_c$  is mean collisional time or mean free path of the interacting medium. It is Fourier's transformation, which can connect between  $M$ -axis and  $t$ -axis, hence,  $\delta(M - M_0)$  and  $1$  are linked in non-interacting picture, while  $\rho(M)$  and  $e^{-t/\tau_c}$  are linked in interacting picture. We see that due to interaction, finite  $\Gamma_c$ ,  $\tau_c$ ,  $\lambda_c$  are expected and therefore, probability of particle with time/position will be exponentially reduced. Similar to limiting case (16), one can get back constant probability in time/position space for  $\Gamma_c \rightarrow 0$  as

$$\lim_{\Gamma_c \rightarrow 0} e^{-t/\tau_c} \rightarrow 1. \quad (17)$$

So, transforming the expressions from  $\Gamma_c \rightarrow 0$  or  $\tau_c \rightarrow \infty$  to finite  $\Gamma_c$  or  $\tau_c$ , one can build non-interacting to interacting picture description. Following that, if delta functions in Eq. (14) will be replaced by their corresponding  $\rho(M)$ 's with  $M_0 = 0, m_u, m_s$  for gluon, u/d quark and s quark, then non-interacting to interacting energy density expressions can be obtained. Applying same technique to Eq. (2) and then in Eq. (4), one finally get  $s$  of interacting system, where  $\Gamma_c$  parameter can be tuned to match LQCD data [44, 45]. By this matching, we get parametrized of  $\Gamma_c(T)$ :

$$\Gamma_c(T) = a_0 - \frac{a_1}{e^{a_2(T-a_3)} + a_4} \quad (18)$$

where,  $a_0 = 6.76802$ ,  $a_1 = 88.6265$ ,  $a_2 = -37.3715$ ,  $a_3 = 0.170$ ,  $a_4 = 14.0653$ . It is plotted in Fig. 3(a) and corresponding  $s/T^3$  is displayed in Fig. 3(b). In hadronic temperature range,  $\Gamma_c(T)$  decreases with  $T$  but it saturates with the values  $\Gamma_c \approx 0.500$  GeV in quark temperature domain. Here, one can again find set-2 parametrization of  $\Gamma_c(T)$ , where  $\Gamma_c \rightarrow 0$  at  $T \rightarrow \infty$  but that choice provide a very bad matching of LQCD data, so we have not considered that set.

### 3 Estimation of shear viscosity and electrical conductivity

After developing different alternative ways to build a quasi-particle model, which match well the LQCD data of QGP thermodynamics, here, we will plug in that QCD interaction in calculations of different transport coefficients like shear viscosity ( $\eta$ ) and electrical conductivity ( $\sigma$ ). We know that quasi-particle expressions of  $\eta$  and  $\sigma$ , addressed in Appendix/Sec. (5), can be obtained from either relaxation time approximation (RTA) of kinetic theory [47, 46, 37] or from one-loop diagram of respective correlators, based on Kubo relations [48, 49, 50, 51]. Interestingly both methodology provide same final expressions for different transport coefficients because of their own approximations. The detail derivation of the final expressions of  $\eta$ ,  $\sigma$  from two methodology are described in Appendix/Sec. (5). Let us start here from directly final expressions for QGP system,

$$\begin{aligned} \eta_t &= \sum_{i=g,u,s} \eta_i \\ &= \frac{g_g}{15T} \int \frac{d^3 \vec{p}}{(2\pi)^3} \vec{p}^2 \tau f(1+f) + \frac{g_u}{15T} \int \frac{d^3 \vec{p}}{(2\pi)^3} \left( \frac{\vec{p}^2}{\omega_u} \right)^2 \tau f(1-f) \\ &\quad + \frac{g_s}{15T} \int \frac{d^3 \vec{p}}{(2\pi)^3} \left( \frac{\vec{p}^2}{\omega_s} \right)^2 \tau f(1-f) \end{aligned} \quad (19)$$

$$\begin{aligned} \sigma_t &= \sum_{i=u,s} \sigma_i \\ &= \frac{e_u^2 g_e}{3T} \int \frac{d^3 \vec{p}}{(2\pi)^3} \left( \frac{\vec{p}}{\omega_u} \right)^2 \tau f(1-f) + \frac{e_s^2 g_e}{3T} \int \frac{d^3 \vec{p}}{(2\pi)^3} \left( \frac{\vec{p}}{\omega_s} \right)^2 \tau f(1-f) . \end{aligned} \quad (20)$$

Gluons are uncharged and hence do not contribute to electrical conductivity. The above the Eqs. (19), (20) in massless limit (i.e.  $m_{u,s} \rightarrow 0$ ) will convert to a simple analytic function,

$$\begin{aligned} \eta_t &= \left[ g_g + \left( \frac{7}{8} \right) (g_u + g_s) \right] \frac{4\tau}{5\pi^2} \zeta(4) T^4 = \left[ 16 + \left( \frac{7}{8} \right) (24 + 12) \right] \frac{4\tau}{5\pi^2} \zeta(4) T^4 \\ \sigma_t &= (e_u^2 g_e + e_s^2 g_e) \frac{\tau}{3\pi^2} \zeta(2) T^2 = \left[ 12 \left( \frac{5e^2}{9} \right) + 12 \left( \frac{e^2}{9} \right) \right] \frac{\tau}{3\pi^2} \zeta(2) T^2 \end{aligned} \quad (21)$$

where  $\zeta(4) = \pi^4/90$ ,  $\zeta(2) = \pi^2/6$ . So we will get massless limit of transport coefficients,  $\eta_t/(\tau T^4) \approx 4.16$  and  $\sigma_t/(2\tau T^2) \approx 0.22e^2 \approx 0.02$  as we have found similar type (SB) limiting values for thermodynamical quantity  $s/T^3 \approx 20.8$ . We have plotted  $\eta_t/(\tau T^4)$  vs  $T$  and  $\sigma_t/(2\tau T^2)$  vs  $T$  curves (brown dotted line) in Fig. 4(a) and (b), which should be exactly straight horizontal line for massless case but actually it will not because of finite values of  $m_u$  and  $m_s$ . So, for non-interacting picture, we are getting roughly constant values of  $\eta_t/(\tau T^4)$

and  $\sigma_t/(2\tau T^2)$ , which can be modified in interacting picture. As we noticed in earlier section, we have attempted to build interaction picture of QGP system by introducing temperature dependent (1) degeneracy factor  $g(T)$ , (2) fugacity  $Z(T)$  and (3) thermal width  $\Gamma_c(T)$ . Implementing them one by one, we will estimate their corresponding values of transport coefficients.

Let us first come to temperature dependent degeneracy factor case. Multiplying  $g(T)$  of Eq. (8) with  $g_{g,u,s}$  in Eqs.(19) and (20) , we have obtained the curves, shown by dash line in Fig. 4(a) and (b). Next, we go to the  $Z(T)$  case, where we have modified the distribution function by using  $Z(T)$  and got dash-dotted curves in Fig. 4(a) and (b). Then we have done the third case  $\Gamma_c(T)$ . Here, we have to first replace energy of gluons, quarks as  $\sqrt{\vec{p}^2 + M^2}$  in Eqs. (19) and (20) and then we have to integrate by their respective spectral function  $\rho(M)$ 's. So the modified expressions of Eqs. (19) and (20) will be

$$\begin{aligned} \eta_t &= \sum_{i=g,u,s} \eta_i \\ &= \frac{g_g}{15T} \int \frac{dM}{\pi} \left( \frac{\Gamma_c}{\Gamma_c^2 + M^2} \right) \int \frac{d^3 \vec{p}}{(2\pi)^3} \frac{\vec{p}^4}{\vec{p}^2 + M^2} \tau f(1+f) \\ &+ \frac{g_u}{15T} \int \frac{dM}{\pi} \left( \frac{\Gamma_c}{\Gamma_c^2 + (M - m_u)^2} \right) \int \frac{d^3 \vec{p}}{(2\pi)^3} \frac{\vec{p}^4}{\vec{p}^2 + M^2} \tau f(1-f) \\ &+ \frac{g_s}{15T} \int \frac{dM}{\pi} \left( \frac{\Gamma_c}{\Gamma_c^2 + (M - m_s)^2} \right) \int \frac{d^3 \vec{p}}{(2\pi)^3} \frac{\vec{p}^4}{\vec{p}^2 + M^2} \tau f(1-f) \end{aligned} \quad (22)$$

$$\begin{aligned} \sigma_t &= \sum_{i=u,s} \sigma_i \\ &= \frac{e_u^2 g_e}{3T} \int \frac{dM}{\pi} \left( \frac{\Gamma_c}{\Gamma_c^2 + (M - m_u)^2} \right) \int \frac{d^3 \vec{p}}{(2\pi)^3} \frac{\vec{p}^2}{\vec{p}^2 + M^2} \tau f(1-f) \\ &+ \frac{e_s^2 g_e}{3T} \int \frac{dM}{\pi} \left( \frac{\Gamma_c}{\Gamma_c^2 + (M - m_s)^2} \right) \int \frac{d^3 \vec{p}}{(2\pi)^3} \frac{\vec{p}^2}{\vec{p}^2 + M^2} \tau f(1-f) . \end{aligned} \quad (23)$$

The green solid lines in Figs. 4(a) and (b) is showing the respective transport coefficients curves, where QCD interaction has been mapped through temperature dependent thermal width, given in Eq. (18). So from the dash, dash-dotted and solid line curves of Figs. 4(a) and (b), based on  $g(T)$ ,  $Z(T)$  and  $\Gamma_c(T)$  parameterizing quasi-particle models, we notice a common qualitative message - transport coefficients of non-interacting QGP will be reduced because of interaction as noticed in thermodynamical quantity like  $s$ .

Seeing the reduction in thermodynamical phase-space of shear viscosity in interaction picture, we have inclined to search - is there any dominant/partial/non-negligible role of interaction for reducing fluidity of QGP, for which we are getting a (nearly) perfect fluid system? However, instead of  $\eta$  only, we should found the dimensionless ratio  $\eta/s$ , which basically measures the fluidity of a system. Since  $\eta$  and  $s$  both are facing reduction due to interaction, so it is not straight forward to make a comment about the role of interaction on QGP fluidity. We have plotted first  $\eta/s$  for non-interaction system by using  $\tau = 1$  and 10 fm, shown by solid line in Fig. 5(a). Then generated same curves for  $g(T)$ ,  $Z(T)$  based quasi-particle model and interestingly, we have found those interacting curves are exactly coincided with non-interacting curves. It reflects that the quantity  $g(T)$  and  $Z(T)$  in  $\eta$ ,  $s$ , which map QCD interaction, are exactly canceled in ratio  $\eta/s$ . Therefore,  $\eta/s$  for non-interacting and interacting QGP system, based on  $g(T)$  and  $Z(T)$  parametrization are

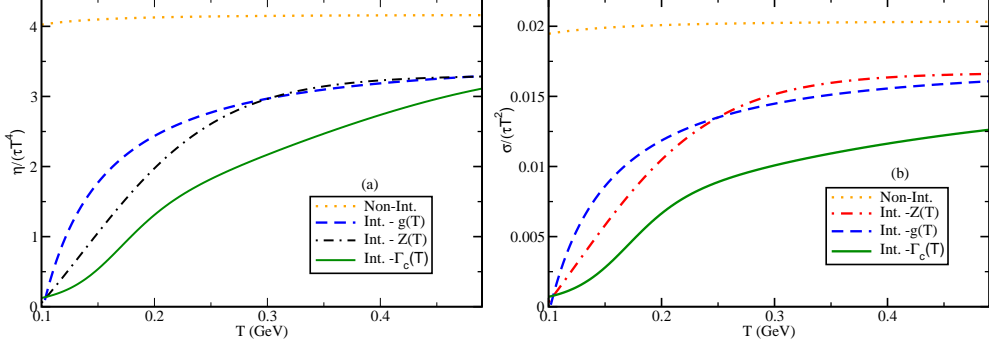


Figure 4: Temperature dependent of (a)  $\eta/(\tau T^4)$ , (b)  $\sigma/(\tau T^2)$  are plotted by using temperature dependent degeneracy factor  $g(T)$  (dash line), fugacity  $Z(T)$  (dash-dotted line) and thermal width  $\Gamma_c(T)$  (solid line). Horizontal dotted lines indicate corresponding non-interacting values.

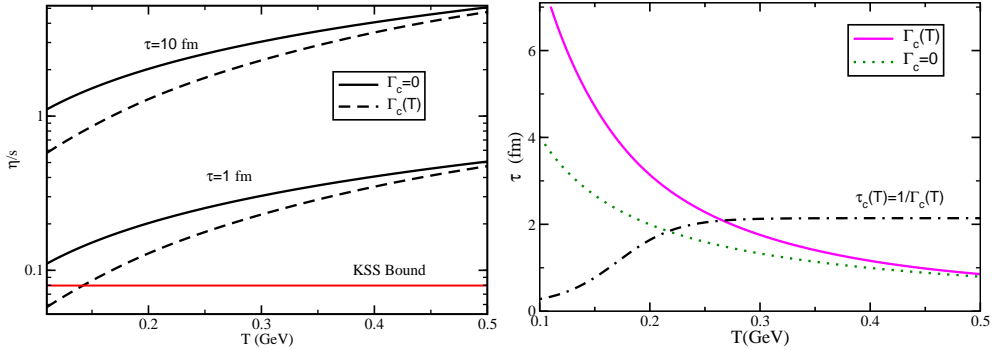


Figure 5: (a)  $\eta/s$  vs  $T$  for non-interacting (solid line) and interacting (dash line) cases by considering  $\Gamma_c = 0$  and  $\Gamma_c(T)$ . Curves are plotted for two values of relaxation time. (b) By imposing  $\eta/s = 1/(4\pi)$ ,  $\tau(T)$  has been found for non-interacting or  $\Gamma_c = 0$  (dotted line) and interacting or  $\Gamma_c(T)$  (solid line) cases. The  $\tau_c(T) = 1/\Gamma_c(T)$  is also plotted to compare with relaxation time scale  $\tau$ .

exactly same. However, this picture is not true in  $\Gamma_c(T)$  parametrization. The dash lines in Fig. 5(a) show the interacting curves of  $\eta/s$ , based on  $\Gamma_c(T)$  parametrization for  $\tau = 1$  and 10 fm. We notice a clear reduction of  $\eta/s$  i.e. fluidity of QGP because of interaction.

Now, relaxation time  $\tau$  in the expression of shear viscosity and electrical conductivity keep as free parameter and in principle it is different from particle collisional time  $\tau_c = 1/\Gamma_c$ . By definition, relaxation time is the time scale, required to return from non-equilibrium to equilibrium distribution function. Now, this non-equilibrium state can be created either by shear stress or by electrical field and because of different sources of dissipative forces, relaxation time of different transport coefficients might be different. However, for simplicity we consider that all of them are same. Now this relaxation time  $\tau$  for shear stress can map the interaction of dissipative QGP fluid while quasi-particle collisional time  $\tau_c$  is mapping LQCD thermodynamic. To search connection between them, we have first plotted  $\tau_c(T)$  by dash-dotted line in Fig. 5(b). While, free parameter  $\tau$  in  $\eta$  can be guessed from experimental data of QGP fluid, which indicates about its perfect fluid nature i.e.  $\eta/s$  touch the KSS value  $1/(4\pi)$ . So imposing  $\eta/s = 1/(4\pi)$  for non-interacting and interacting picture, based on  $\Gamma_c(T)$  parametrization, we have generated dotted and solid lines respectively in Fig. 5(b). For non-interacting and massless case (i.e.  $m_{u,s} \rightarrow 0$ ), we get simplest relation

$$\begin{aligned} \frac{\eta}{s} &= \frac{1}{4\pi} \\ \Rightarrow \frac{\tau T}{5} &= \frac{1}{4\pi} \\ \Rightarrow \tau &= \frac{5}{4\pi T}, \end{aligned} \quad (24)$$

although it will be little different for  $m_u = 0.005$  GeV and  $m_s = 0.100$  GeV. For interaction case, we will not get any analytic expression as a clue, rather we have to follow the numerical values of solid lines of Fig. 5(b) to understand the trend.

Let us try to relate these two time scale roughly as  $\tau = \phi(T)\tau_c$ , where  $\phi(T) < 1$  for quark temperature domain and  $\phi(T) > 1$  for hadronic temperature domain are noticed in Fig. 5(b). If we roughly understand larger time scale as more macroscopic, then at quark temperature domain,  $\tau_c$  is appeared as macroscopic scale, whereas at hadronic temperature domain  $\tau$  plays the macroscopic role. In general, for good kinetic theory approximation, we consider  $\tau \approx \tau_c$ , which might be more or less applicable near and above transition temperature at least in order of magnitude ( $\tau_c \approx 2$  fm,  $\tau \approx 1$  fm). It indicates that high temperature QCD interaction time scale, covered by LQCD data is quite well agreement with shear dissipative interaction of QGP, although this equivalence might not be true in low temperature hadronic phase.

## 4 Summary

Present article has attempted to build three different possible quasi-particle models to map the QCD interaction from LQCD simulation. We have shown that by introducing a temperature dependent (1) degeneracy factors, (2) fugacity and (3) thermal width of quarks and gluons, one can build the interacting description from non-interacting case, where those quantities had some fixed values. To fit LQCD data of thermodynamics like entropy density, we have found the temperature dependent parametric forms of those quantities. The degeneracy factors and fugacity are appeared as increasing functions, whereas thermal width

come as decreasing function. At infinite temperature, they will reach their extreme limits or the non-interacting values (52, 1, 0 respectively), where thermodynamical quantities merge to their non-interacting values, popularly called SB limits.

After building three different forms of quasi-particle models, we have applied them to estimate transport coefficients like shear viscosity, electrical conductivity of QGP. Similar to the reduction of thermodynamical quantities, transport coefficients also reduce during the transition from non-interacting to interacting picture. The quantitative reduction of transport coefficients from different models are appeared to be different, although their qualitative temperature dependent curves are quite similar. Estimating the shear viscosity to entropy density ratio, we found that non-interacting and interacting results become same for the degeneracy factor and fugacity based models but they are different for thermal width based model. For latter model, we observe that interaction can have some role to reduce the value of shear viscosity to entropy density ratio, which measure the fluid property of medium.

As a future plan, our interest to map QCD interaction in presence of magnetic field through similar type of quasi-particle models, where we can notice the comparative roles of QCD interaction with and without field picture on fluid property of QGP.

**Acknowledgment:** SG acknowledges to MHRD funding via IIT Bhilai and SS acknowledges to facilities, provided from IIT Bhilai in self-sponsor PhD scheme. AA, SP, RK thanks for (payment basis) hospitality from IIT Bhilai during his summer internship tenure (May-June, 2019). RK is supported through KVPY fellowship.

## 5 Appendix

### 5.1 RTA method

Here we will provide a brief framework shear viscosity ( $\eta$ ) and electrical conductivity ( $\sigma$ ), whose modified estimated values due to transition from non-interacting to interacting picture is our matter of interest in present study. Transport coefficients like  $\eta$  and  $\sigma$  are basically non-equilibrium measurements of the system by following the macroscopic relations

$$\begin{aligned} T_\eta^{ij} &= \eta U_\eta^{ij} \\ J_\sigma^i &= \sigma^{ij} E_j , \end{aligned} \quad (25)$$

where  $T^{ij}$  is shear part of energy momentum tensor,  $U_\eta^{ij} = D^i u^j + D^j u^i + \frac{2}{3} \Delta^{ij} \partial_\rho u^\rho$  with  $D^i = \partial^i - u^i u^\sigma \partial_\sigma$  and  $\Delta^{ij} = g^{ij} - u^i u^j$  is velocity gradient component,  $J^i$  is electrical current density due to electric field  $E_j$ . Considering  $\delta f$  deviation from equilibrium distribution function, the Eq. (25) can have microscopic form

$$\begin{aligned} \eta U_\eta^{ij} &= T^{ij} = g \int \frac{d^3 p}{(2\pi)^3} \frac{p^\mu p^\nu}{E} \delta f \\ \sigma^{ij} E_j &= J^i = g_e e \int \frac{d^3 p}{(2\pi)^3} \frac{p^\mu}{E} \delta f , \end{aligned} \quad (26)$$

where  $g$  is degeneracy factors of medium constituents and  $g_e e$  electric charge degeneracy factors (will be discussed latter more elaborately). Considering  $\delta f$  with same tensorial decomposition,

$$\delta f = (A_{ij} U_\eta^{ij} + C_i E^i) f (1 \pm f) , \quad (27)$$

with  $\pm$  stand for bosonic and fermionic medium constituents respectively and the unknown coefficients  $A_{ij}$  and  $C_i$  can be found as

$$A_{ij} = \tau_\eta \frac{\beta p_i p_j}{E} \quad (28)$$

$$C_i = \tau_\sigma \frac{e \beta p_i}{E} \quad (29)$$

by using the relaxation time approximation form of Boltzmann's equation. The  $\tau$  and  $\tau_\sigma$  are relaxation time for shear force and electrical field respectively. Using Eqs. (29), (27) in Eq. (26), we get the final expressions of  $\eta$  and  $\sigma$  for gluons (boson) and quarks (fermion) [47, 46, 37]:

$$\begin{aligned} \eta_{g,Q} &= \frac{g_{g,Q}}{15T} \int \frac{d^3 \vec{p}}{(2\pi)^3} \left( \frac{\vec{p}^2}{\omega} \right)^2 \tau f(1 \pm f) \\ \sigma_Q &= \frac{e_Q^2 g_e}{3T} \int \frac{d^3 \vec{p}}{(2\pi)^3} \left( \frac{\vec{p}}{\omega} \right)^2 \tau f(1 - f) . \end{aligned} \quad (30)$$

Considering  $g_g = 16$ ,  $g_u = 24$ ,  $g_s = 12$  and  $e_u^2 g_e = 12 \times \frac{5e^2}{9}$ ,  $e_s^2 g_e = 12 \times \frac{e^2}{9}$  and  $\omega = \vec{p}$ ,  $\sqrt{\vec{p}^2 + m_u^2}$ ,  $\sqrt{\vec{p}^2 + m_s^2}$  for  $g$ ,  $u$  and  $s$ , we can get total contribution of QGP as

$$\begin{aligned} \eta_t &= \eta_u + \eta_s + \eta_g \\ \sigma_t &= \sigma_u + \sigma_s \end{aligned} \quad (31)$$

## 5.2 Kubo relation

Apart from RTA method, one can obtain same expressions, given in Eq. (30), from alternative technique, commonly known as Kubo relation. It starts with basic definition, where any transport coefficients  $\mathcal{T}$  can be expressed in terms of thermal correlator of relevant operator  $\mathcal{O}$  by a proportional relation. For  $\mathcal{T} = \eta, \sigma$ , operators are  $T_\eta^{\mu\nu}$  and  $J_\sigma^\mu$ , given in Eqs. (25), and their connecting Kubo relations are [48, 49, 50, 51]

$$\begin{aligned} \eta &= \frac{1}{20} \lim_{q_0, \vec{q} \rightarrow 0} \frac{A_\eta(q_0, \vec{q})}{q_0} \\ \sigma &= \frac{1}{6} \lim_{q_0, \vec{q} \rightarrow 0} \frac{A_\sigma(q_0, \vec{q})}{q_0} , \end{aligned} \quad (32)$$

where

$$\begin{aligned} A_\eta(q_0, \vec{q}) &= \int d^4 x e^{iqx} \langle [T_{\mu\nu}(x), T^{\mu\nu}(0)] \rangle \\ A_\sigma(q_0, \vec{q}) &= \int d^4 x \langle [J_\mu(x), J^\mu(0)] \rangle . \end{aligned} \quad (33)$$

From free Lagrangian density of quarks (fermion) and gluons (bosons), one can know

$$\begin{aligned} T_{\mu\nu} &= \left( \Delta_\mu^\rho \Delta_\nu^\sigma - \frac{\Delta_{\mu\nu} \Delta^{\rho\sigma}}{3} \right) (i \bar{\psi} \gamma_\rho \partial_\sigma \psi) \text{ for quark field } \psi \\ &= \left( \Delta_\mu^\rho \Delta_\nu^\sigma - \frac{\Delta_{\mu\nu} \Delta^{\rho\sigma}}{3} \right) (\partial_\rho \phi \partial_\sigma \phi) \text{ for gluon field } \phi , \end{aligned} \quad (34)$$

with  $\Delta_{\mu\nu} = g^{\mu\nu} - u^\mu u^\nu$ . The electric current of quark field  $\psi$  is

$$J_Q^\mu = q_Q \bar{\psi} \gamma^\mu \psi . \quad (35)$$

Using these in Eq. (32), we can express  $\eta$  and  $\sigma$  in terms of field and applying Feynman techniques, we can obtain

$$\begin{aligned} \eta &= \frac{\beta}{5} \int \frac{d^3 \vec{k}}{(2\pi)^3} \frac{N_\eta}{4\omega^2 \Gamma} [f(1 \pm f)] \\ \sigma &= \frac{\beta}{3} \int \frac{d^3 \vec{k}}{(2\pi)^3} \frac{(N_\sigma)}{4\omega^2 \Gamma} [f(1 - f)] \end{aligned} \quad (36)$$

where vertex kind of factor of respective one-loop self-energy diagrams can be obtained as

$$\begin{aligned} N_\eta &= g \frac{4\vec{k}^4}{3} \\ N_\sigma &= g_e 4e_Q^2 \vec{k}^2 \end{aligned} \quad (37)$$

and thermal width  $\Gamma = 1/\tau$  has been introduced in propagators of respective diagrams to cure their divergence near zero momentum. After putting Eq. (37) in Eq. (36), one can return to Eq. (30). So we can get same final expressions of  $\eta$ ,  $\sigma$  from either kinetic theory of RTA method or Kubo-type (one-loop) diagrammatic method.

## References

- [1] F. Karsch, *Lattice QCD at finite temperature: a status report*, Zeitschrift Fur Physik **C 38**, 147 (1988).
- [2] S. Sharma, *QCD Thermodynamics on the Lattice* AHEP 2013, 452978 (2013).
- [3] M. Strickland, J. O. Andersen, L. E. Leganger, N. Su, *Hard-thermal-loop QCD Thermodynamics* Prog. Theor. Phys. Suppl. 187, 106 (2011).
- [4] J. O. Andersen, M. Strickland, and N. Su, *Gluon Thermodynamics at Intermediate Coupling* Phys. Rev. Lett. 104, 122003 (2010).
- [5] J. O. Andersen, M. Strickland, and N. Su, *Three-loop HTL gluon thermodynamics at intermediate coupling* JHEP 1008, 113 (2010).
- [6] N. Haque, A. Bandyopadhyay, J. O. Andersen, M. G. Mustafa, M. Strickland, N. Su, *Three-loop HTLpt thermodynamics at finite temperature and chemical potential*, JHEP 1405 (2014) 027.
- [7] N. Haque, J. O. Andersen, M. G. Mustafa, M. Strickland, N. Su, *Three-loop pressure and susceptibility at finite temperature and density from hard-thermal-loop perturbation theory*, Phys. Rev. **D 89** (2014) 061701.
- [8] A.N. Tawfik, *Equilibrium Statistical-Thermal Models in High-Energy Physics* Int. J. Mod. Phys. A 29 (2014), 1430021.

- [9] S.P. Klevansky, *The Nambu-Jona-Lasinio model of quantum chromodynamics* Rev. Mod. Phys. 64 (1992) 649.
- [10] T. Hatsuda, T. Kunihiro *QCD phenomenology based on a chiral effective Lagrangian* Phys. Rept. 247 (1994) 221.
- [11] M. Buballa, *NJL model analysis of quark matter at large density* Phys. Rept. 407 (2005) 205.
- [12] Mark I. Gorenstein, Shin Nan Yang, *Gluon plasma with a medium-dependent dispersion relation*, Phys. Rev. **D 52**, 5206 (1995).
- [13] A.Peshier, B.Kampfer, O.P. Pavlenko, G. Soff, *Massive quasiparticle model of the  $SU(3)$  gluon plasma* Phys. Rev. **D 54** (1996)
- [14] P. Levai and U. W. Heinz, *Massive gluons and quarks and the equation of state obtained from  $SU(3)$  lattice QCD* Phys. Rev. C 57, 1879 (1998).
- [15] M. Bluhm, B. Kämpfer, and G. Soff, *The QCD equation of state near  $T_c$  within a quasi-particle model* Phys. Lett. B 620, 131 (2005).
- [16] V.M. Bannur, *Self-consistent quasiparticle model for quark-gluon plasma* Phys. Rev. **C 75**, 044905 (2007).
- [17] Salvatore Plumari, Wanda M. Alberico, Vincenzo Greco, Claudia Ratti, *Recent thermodynamic results from lattice QCD analyzed within a quasiparticle model* Phys. Rev. **84**, 094004 (2011).
- [18] P. N. Meisinger, M. C. Ogilvie, and T. R. Miller, *Gluon Quasiparticles and the Polyakov Loop* Phys. Lett. B 585, 149 (2004).
- [19] M. Ruggieri, P. Alba, P. Castorina, S. Plumari, C. Ratti, V. Greco, *Polyakov loop and gluon quasiparticles in Yang-Mills thermodynamics* Phys. Rev. **D 86**, 054007 (2012).
- [20] V. Chandra, R. Kumar, V. Ravishankar, *Hot QCD equations of state and relativistic heavy ion collisions* Phys. Rev. **C 76** (2007) 054909.
- [21] Vinod Chandra, V. Ravishankar, *Quasi-particle model for lattice QCD: Quark-gluon plasma in heavy ion collisions*, Eur. Phys. J. **C 64** (2009) 63.
- [22] V. Chandra, V. Ravishankar, *A quasi-particle description of (2+1)- flavor lattice QCD equation of state* Phys. Rev. **D 84**, 074013 (2011).
- [23] PHENIX collaboration, S. S. Adler et al., Phys. Rev. Lett. 91 (2003) 182301,nucl-ex/0305013; STAR collaboration, J. Adams et al., Phys. Rev. **C 72** (2005) 014904, nucl-ex/0409033.
- [24] ALICE collaboration, K. Aamodt et al., Phys. Rev. Lett. 107(2011) 032301, nucl-ex/1105.3865; CMS collaboration, S. Chatrchyan et al., Phys. Lett.B 724 (2013) 213, nucl-ex/1305.0609; ATLAS collaboration, G. Aad et al., Phys. Rev. **C 90** (2014) 024905, hep-ex/1403.0489.

[25] S. Ghosh, T. C. Peixoto, V. Roy, F. E. Serna, G. Krein, *Shear and Bulk Viscosities of Quark Matter from Quark-Meson Fluctuations in the Nambu-Jona-Lasinio model*, Phys. Rev. **C 93** (2016) 045205, nucl-th/1507.08798.

[26] S. Ghosh, F. E. Serna, A. Abhishek, G. Krein, H. Mishra, *Transport responses from rate of decay and scattering processes in the Nambu-Jona-Lasinio model* Phys. Rev. **D 99** (2019) 014004, nucl-th/1809.07594.

[27] S. Ghosh, A. Lahiri, S. Majumder, R. Ray, S. K. Ghosh, *Shear viscosity due to Landau damping from the quark-pion interaction* Phys. Rev. C **88**, 068201 (2013),nucl-th/1311.4070.

[28] R. Lang and W. Weise, *Shear viscosity from Kubo formalism: NJL model study*, Eur. Phys. J. A **50**, 63 (2014), hep-ph/1311.4628.

[29] R. Lang, N. Kaiser, and W. Weise, *Shear viscosities from Kubo formalism in a large- $N_c$  Nambu-Jona-Lasinio model* Eur. Phys. J. A **51**, 127 (2015), hep-ph/1506.02459.

[30] P. Zhuang, J. Hufner, S.P. Klevansky, L. Neise, *Transport properties of a quark plasma and critical scattering at the chiral phase transition* Phys. Rev. D **51**, 3728 (1995).

[31] P. Rehberg, S.P. Klevansky and ,J. Hufner, *Elastic Scattering and Transport Coefficients for a Quark Plasma in  $SU_f(3)$  at Finite Temperatures* Nucl. Phys. A **608**, 356 (1996), hep-ph/9607263.

[32] C. Sasaki, K. Redlich, *Transport coefficients near chiral phase transition*, Nucl. Phys. A **832** (2010) 62, hep-ph/0811.4708.

[33] P. Deb, G. Kadam, H. Mishra, *Estimating transport coefficients in hot and dense quark matter*, Phys. Rev. D **94** (2016) 094002, hep-ph/1603.01952.

[34] A. Abhishek, H. Mishra, S. Ghosh, *Transport coefficients in the Polyakov quark meson coupling model: A relaxation time approximation*, Phys. Rev. D **97** (2018) 014005, hep-ph/1709.08013

[35] P. Singha, A. Abhishek, G. Kadam, S. Ghosh, H. Mishra, *Calculations of shear, bulk viscosities and electrical conductivity in the Polyakov-quark-meson model* J. Phys. G **46** (2019) 015201, nucl-th/1705.03084.

[36] S. K. Ghosh, S. Raha, R. Ray, K. Saha, S. Upadhyaya, *Shear viscosity and phase diagram from Polyakov-Nambu-Jona-Lasinio model*, Phys. Rev. D **91** (2015) 054005, hep-ph/1411.2765.

[37] C.A. Islam, J. Dey, S. Ghosh [arXiv:1901.09543]

[38] R. Marty, E. Bratkovskaya, W. Cassing, J. Aichelin, H. Berrehrah, *Transport coefficients from the Nambu-Jona-Lasinio model for  $SU(3)_f$* , Phys. Rev. C **88** (2013) 045204, hep-ph/1311.3159.

[39] S. Plumari, A. Puglisi, F. Scardina and V. Greco, *Shear Viscosity of a strongly interacting system: Green-Kubo vs. Chapman-Enskog and Relaxation Time Approximation*, Phys. Rev. C **86** (2012) 054902.

- [40] Vinod Chandra, V. Ravishankar, *Viscosity and thermodynamic properties of QGP in relativistic heavy ion collisions* Eur. J. Phys. **C 59** (2009), 705, [arXiv:0805.4820 [nucl-th]].
- [41] Vinod Chandra, Sukanya Mitra, *Transport coefficients of a hot QCD medium and their relative significance in heavy-ion collisions* Phys. Rev. **D 96**, 094003 (2017).
- [42] Vinod Chandra, Sukanya Mitra, *Thermal relaxation, electrical conductivity, and charge diffusion in a hot QCD medium* Phys. Rev. **D 94** (2016) 034025.
- [43] Vinod Chandra, Sukanya Mitra, *Covariant kinetic theory for effective fugacity quasi-particle model and first order transport coefficients for hot QCD matter* Phys. Rev. **D 97**, 034032 (2018).
- [44] S. Borsanyi et. al., *Full result for the QCD equation of state with 2+1 flavors* Phys. Lett. **B 370** (2014) 99, arXiv:1309.5258 [hep-lat].
- [45] A. Bazavov et al. *Equation of state in (2+1)-flavor QCD* Phys. Rev. D 90, 094503 (2014)
- [46] P. Chakraborty and J. I. Kapusta, Phys. Rev. C **83**, 014906 (2011).
- [47] S. Gavin, *Transport Coefficients In Ultrarelativistic Heavy Ion Collisions*, Nucl. Phys. **A 435**, 826 (1985).
- [48] D. Fernandez-Fraile and A. Gomez Nicola, Eur. Phys. J. **C 62**, 37 (2009).
- [49] S. Jeon, Phys. Rev. D 52, 3591 (1995).
- [50] S. Ghosh, Int. J. Mod. Phys. A 29, 1450054 (2014).
- [51] S. Ghosh, *Electrical conductivity of hadronic matter from different possible mesonic and baryonic loops*, Phys. Rev. **D 95**, 036018 (2017).